

Temporal Analysis of Products (TAP) Study of the Adsorption of CO, O_2, and CO_2 on a Au/Ti$(OH)_4$* Catalyst

Maria Olea,# Maki Kunitake, Takafumi Shido, Kiyotaka Asakura,## and Yasuhiro Iwasawa*

Department of Chemistry, Graduate School of Science, The University of Tokyo, Hongo, Bunkyo-ku, Tokyo 113-0033

(Received July 19, 2000)

The adsorption kinetics on Au/Ti$(OH)_4$* (a newly developed Au catalyst, active for low-temperature CO oxidation) for CO, O_2, and CO_2 in the temperature range 298–473 K was determined by temporal analysis of products (TAP) technique. The response signals from the single-pulse TAP experiments were analyzed using a statistical approach, and they were fitted to analytical models in order to establish the adsorption/desorption parameters. The pulse response of a non-adsorbing gas (argon) was used as a "reference". The experiments revealed that: CO molecules reversibly adsorbed on the catalyst surface; O_2 molecularly adsorbed , irreversibly for high pulse intensities and reversibly for low pulse ones; CO_2 molecules irreversibly adsorbed on the surface, probably as carbonates. This catalyst exhibited an apparent negative activation energy for irreversible adsorption of O_2.

A "temporal analysis of products (TAP)" reactor system was introduced in 1986–1988 as a novel system to study the kinetics and mechanism of heterogeneous catalytic reactions by a pulsed transient response technique with sub millisecond time resolution.[1,2] The high time-resolution of the TAP reactor system is achieved by the use of high-speed pulse valves, a near-zero dead volume manifold, and a catalytic micro-reactor placed directly inside a high-vacuum mass spectrometer detection chamber.[3] The TAP method has found wide applications to heterogeneous catalysis. Up to now, TAP studies on mechanisms of catalytic reactions,[3–18] adsorption on catalyst surfaces,[18–20] and modeling of TAP reactors[22–30] have been reported. Transient experiments have the potential to provide information that cannot be obtained from steady-state experiments. While steady-state experiments give an integrated picture of a reaction system, transient experiments give information on individual steps involved in a catalytic reaction. TAP is a transient technique, but the TAP reactor uses a different experimental strategy for extracting kinetic information from those for other non steady-state techniques such as traditional PFR (plug-flow reactor) and CSTR (continuously stirred tank reactor). In general, the quantification of kinetic parameters from transient measurements requires a well-defined flow mechanism in a micro-reactor and an appropriate model of the system. In the PFR or CSTR systems (classical models used to describe the flow pattern) the pulse of a reactant is introduced into a continuously flowing carrier gas at normal or elevated pressure. The spreading of the pulse often affects axial dispersion in the bed and the adsorption kinetics. The TAP system is different since no carrier gas, such as helium and nitrogen, is used. The TAP strategy is to operate in the Knudsen diffusion regime in which transport is well defined. In this regime, the transport of individual species is independent of the gas composition.[29] A goal of the analysis of the TAP kinetic data is to calculate the kinetic parameters for each elementary step (diffusion, adsorption, chemical reaction, and desorption). This theoretical analysis is based on the reactor model used to describe the behavior of the catalyst bed during the gas pulse. The simplest model is the "one-zone" (the catalyst only zone) reactor model.[25] In order to improve the transport model through the "one-zone" TAP reactor, a symmetrical cylindrical or two-dimensional model has been developed.[27] However, the results demonstrate that the simpler one-dimensional model is as accurate as the two-dimensional model for describing the transport in the TAP reactor.

Another model is the "three-zone" reactor model. In a three-zone reactor, a catalyst zone is sandwiched between two beds of inert particles.[31] This reactor has the advantage that the catalyst zone can be more easily maintained in an isothermal condition.

The newest developed model is the so-called "thin-zone" reactor model.[29] In this reactor type, since the thickness of the catalyst zone is made very small compared to the whole length of the reactor, diffusion can be separated from chemical reaction, and concentration gradients across the catalyst bed can be neglected.

We have used the one-zone TAP reactor model for quantification of the adsorption-desorption kinetic parameters and surface reaction of CO, O_2, and CO_2 on a newly developed TiO_2-supported Au catalyst (denoted as Au/Ti$(OH)_4$*). This newly developed Au catalyst was prepared by supporting a Au-

Department of Chemical Engineering, Faculty of Chemistry and Chemical Engineering, Babes-Bolyai University, 11 Arany Janos St., 3400 Cluj-Napoca, Romania
Catalysis Research Center, Hokkaido University, Kita-ku, Sapporo 060-0811, Japan

phosphine complex as a precursor for Au particles on as-precipitated wet titanium hydroxides as a precursor for TiO_2 support, followed by calcination at 673 K.[32–35] This catalyst exhibits a much higher activity for the low-temperature CO oxidation as compared to a conventional Au/TiO_2 catalyst.[32–35]

Since there is disagreement in the literature about the mechanism of CO oxidation, especially as regards oxygen adsorption on supported gold catalysts,[36–42] we attempted to explain the mechanism of CO oxidation on this new catalyst by means of the TAP technique. In addition, no TAP studies about CO, O_2, and CO_2 adsorption on supported gold catalysts have yet been reported. On the other hand, by fast transient measurements in a TAP reactor it is possible to determine the intrinsic property of a species at the catalyst surface in one single pulse experiment.[43]

Theoretical TAP Analysis

The kinetics of transport processes that occur in the TAP pulse response experiments can be described using either a stochastic or a deterministic approach,[25] and the modeling/fitting problem can be divided into three parts: gas flow, gas/solid interaction, and chemical reaction.

The first theoretical work on the TAP system was reported by Gleaves et al.[2,44] A generalized mathematical model is proposed to describe the transport of a gas pulse under vacuum conditions through a fixed-bed micro-reactor. Here, a particular case where a single pulse valve is used to introduce a binary gas mixture in which one of the components can undergo reversible adsorption on the catalyst surface is considered. The equations which describe the transport of a gas pulse, based on mass balance equations, are similar to those used for fixed-bed chromatography, except that no convective terms are present and Knudsen diffusion dominates at sufficiently low pressures.

Therefore, assuming Knudsen flow and first-order adsorption/desorption kinetics, the model is described by Eqs. 1 and 2. Terms and symbols used in the Eqs. are listed in Notation at the end of the text.

$$\frac{\partial C_A}{\partial t} = D_{eA}\frac{\partial^2 C_A}{\partial x^2} - \frac{\rho_s}{\varepsilon_b}k_{aA}C_A(1-\theta_A) + \frac{\rho_s}{\varepsilon_b}k_{dA}\theta_A \qquad (1)$$

$$\frac{\partial \theta_A}{\partial t} = k_{aA}C_A(1-\theta_A) - k_{dA}\theta_A \qquad (2)$$

The initial and boundary conditions are:

$$0 \le x \le L, \qquad t = 0, \qquad C_A = \delta_x \frac{N_{pA}}{\varepsilon_b A} \qquad (3)$$

$$x = 0, \qquad \frac{\partial C_A}{\partial x} = 0,$$
$$x = L, \qquad C_A = 0. \qquad (4)$$

An analytical solution for the above mass balance equations with the initial and boundary conditions is obtained by using a linear operator method. Therefore, the flux at the reactor outlet is established as a function of the adsorption and desorption rate constants and the effective Knudsen diffusion coefficient. Since these parameters are unknown, the method of moments was used for the parameter estimation.

The moments m_n of the exit flows F are represented by the set of integral equations:

$$m_n = \int_0^\infty t^n \mathrm{F}(t,L)\mathrm{d}t. \qquad (5)$$

The moments $m_n(x)$ for the flow through any cross section of the reactor at a given axial coordinate are represented by the set of equations[28]:

$$m_n(x) = \int_0^\infty t^n F(t,x)\mathrm{d}t. \qquad (6)$$

Analysis of the zero-th, first, and second moments of a TAP curve will lead to simple relations used to calculate conversion, adsorption and desorption rate constants, and the activation energy for desorption, as follows:

$$X_A = \frac{400}{\pi}\sum_{n=0}^{\infty}\frac{(-1)^n}{(2n+1)+(2n+1)^3/k^*} \qquad (7)$$

where

$$k^* = \left(\frac{2L}{\pi}\right)^2 \frac{\varepsilon_b k_{aA} k_r}{D_{eA}(k_{dA}+k_r)} \qquad (8)$$

and

$$t_{res} = \frac{L^2\varepsilon_b}{2D_{eA}}\left(1+\frac{k_{aA}}{k_{dA}}\right), \qquad (9)$$

where there are only adsorption and desorption without reaction. The first moment can be related to the mean residence time, t_{res}, by the equation:

$$t_{res} = \frac{m_1}{m_0} \qquad (10)$$

Equation 9 shows that t_{res} depends on the ratio of k_{aA} and k_{dA} but not on their absolute values. The absolute second moment, however, depends on the absolute values of k_{aA} and k_{dA}:

$$\frac{m_2}{m_0} = \frac{2^7 L^4 {\varepsilon_b}^4}{\pi^5 {D_{eA}}^4}(1+\frac{k_{aA}}{k_{dA}})^2 + \frac{\varepsilon_b L^2 k_{aA}}{D_{eA}{k_{dA}}^2} \qquad (11)$$

for the case of no reaction. Another useful equation is given for the peak time in the case of only diffusion:

$$t_p = \frac{t_{res}}{3} = \frac{L^2\varepsilon_b}{6D_{eA}}. \qquad (12)$$

t_p is the time at which the exit flow is at maximum, and can be determined by setting the derivative of the exit flow equation equal to zero.

This model was successfully applied to describe the adsorption-desorption processes in the selective oxidation of propene to acrolein on a Bi_2MoO_6 catalyst.[2] However, many points related to the appropriate boundary conditions for the

micro-reactor remained unclarified. For this reason, the basic model proposed by Gleaves et al. has been developed by Zou, Dudukovič and Mills.[22] The developed model provides the foundation for quantification of results obtained in the TAP system and appropriate boundary conditions for modeling have been sought in their study.

Other results on modeling of the TAP reactor have been published by Greten et al.,[3] Huinink,[45] and Zou et al..[23] But, in their models basically analytical techniques have been applied to solve the model equation. This limits their applicability to the cases where changes in the degree of coverage are negligible and all reactions are of the first-order.

To solve the mathematical model, a more suitable and numerical technique was used by Rothamael and Baerns.[24] In this way, the rate constants for adsorption, desorption and reaction have been determined.

However, since we assume the first-order kinetics for adsorption/desorption of CO, O_2, and CO_2 over Au/Ti(OH)$_4$*, in our TAP analysis we have especially used the theoretical results published by Gleaves et al. in 1997.[25] Moreover, since our TAP reactor is completely filled with a single catalyst sample, our approach is based on the "one-zone-model". Therefore, firstly, we had to verify if the flow in the TAP reactor is in the Knudsen regime.

The equation of the standard diffusion curve has been obtained by solving the equation of continuity for a non-reacting gas in a fixed-bed reactor under the initial and boundary conditions (Eqs. 3 and 4) :

$$\varepsilon_b \frac{\partial C_A}{\partial t} = D_{eA} \frac{\partial^2 C_A}{\partial x^2}. \tag{13}$$

As the gas flow at the reactor exit, F_A , is described by

$$F_A = -AD_{eA} \left.\frac{\partial C_A}{\partial x}\right|_{x=L}, \tag{14}$$

the equation of the standard normalized curve can be written in the following form:

$$\frac{F_A}{N_{pA}} = \frac{D_{eA}\pi}{\varepsilon_b L^2} \sum_{n=0}^{\infty} (-1)^n (2n+1) \times \exp\left(-(n+0.5)^2 \pi^2 \frac{tD_{eA}}{\varepsilon_b L^2}\right). \tag{15}$$

Equation 15 indicates that the normalized flow does not depend on the intensity of the gas pulse. Other properties are shown by the following equations:

$$H_p = 1.85 \frac{D_{eA}}{\varepsilon_b L^2}, \tag{16}$$

$$H_p t_p = 0.31. \tag{17}$$

Equation 17 is a useful criterion for the Knudsen regime. It shows that for an inert gas the product of the normalized peak height and the peak time is constant, regardless of the particle size, temperature or the effective Knudsen diffusivity of the gas.

If an irreversible adsorption/reaction occurs during the TAP experiment, we have to consider the following mass balance for the gas phase component A:

$$\varepsilon_b \frac{\partial C_A}{\partial t} = D_{eA} \frac{\partial^2 C_A}{\partial x^2} - a_s S_v (1-\varepsilon_b) k_{aA} C_A. \tag{18}$$

The apparent adsorption/reaction rate constant, k'_{aA}, is defined as:

$$k'_{aA} = \frac{a_s S_V (1-\varepsilon_b) k_{aA}}{\varepsilon_b}. \tag{19}$$

The initial and boundary conditions for Eq. 18 are the same as those for Eqs. 1 and 2. The equation of flow at the exit is given by:

$$\frac{F_A}{N_{pA}} = \frac{D_{eA}\pi}{\varepsilon_b L^2} \exp(-k'_{aA} t) \sum_{n=0}^{\infty} (-1)^n (2n+1) \times \exp\left(-(n+0.5)^2 \pi^2 \frac{tD_{eA}}{\varepsilon_b L^2}\right). \tag{20}$$

The adsorption rate constant can be determined from the zero-th moment of the normalized flow (which is the same as the zero-th moment of dimensionless flow, $\overline{m}_0$). The zero-th moment of Eq. 20 is given by:

$$m_0 = \overline{m}_0 = \pi \sum_{n=0}^{\infty} \frac{(-1)^n (2n+1)}{(n+0.5)^2 \pi^2 + \overline{k}_a}, \tag{21}$$

where

$$\overline{k}_a = k'_{aA} \frac{\varepsilon_b L^2}{D_{eA}}. \tag{22}$$

Equation 21 can be expressed in another form, which is more useful for determination of the adsorption rate constant, as follows:

$$m_0 = \frac{1}{\cos h \sqrt{\overline{k}_a}}. \tag{23}$$

The conversion, X_A, or fraction of the gas irreversibly adsorbed is described by:

$$X_A = 1 - m_0. \tag{24}$$

As a fingerprint for the irreversible adsorption, the flow curve is situated inside the standard diffusion curve.

When the diffusion + reversible adsorption occurs, the mass balances of a component A in the gas phase, and on the catalyst are described by Eqs. 1 and 2. By solving these equations, the equation of exit flow has been determined. However, more useful for our study was the fingerprint for this case. In contrast to the case of irreversible adsorption, the exit flow curve for the diffusion + reversible adsorption will cross the exit flow for diffusion only. The point at which the curves intersect depends on the adsorption and desorption rate constants.

Experimental

Catalyst. The newly developed catalyst Au/Ti(OH)$_4$* which is highly active for CO oxidation used in our measurements has been described in detail elsewhere.[32–35]

Apparatus. The TAP reactor system has been described in detail elsewhere.[2] We provide here only a brief description as fol-

lows. The TAP system consists of a fast-pulse gas delivery system, a fixed-bed micro-reactor, and a computer-controlled real-time quadrupole mass spectrometer (Spectra Co.). All of them are located in three high-vacuum chambers, the chambers being connected by small pinholes. The base pressures of the chambers are 1, 10^{-6}, and 10^{-8} Pa, respectively. The micro-reactor is made from a stainless steel tube whose diameter and length are 2 and 25 mm, respectively. The catalyst was mounted in the reactor and sandwiched by a stainless steel mesh (40% open). The length of the catalyst in the tube is 10 mm. The reactor was heated by cartilage heaters; the maximum temperature is 773 K. Two pulse valves (General Valve Co.) and a flow line are connected to the reactor, so that transient experiments under gas flow can be done. The minimum pulse width was 200 micro seconds. The flow rate of the gases through the flow line was controlled by thermal mass flow controllers.

TAP Experiments. All experiments were conducted using a pulse mode of operation.[2] Single- pulse transient experiments were performed to investigate the adsorption of the species of interest. In order for the transient output response to be a measure of Knudsen diffusion only, the number of molecules in the input pulse was kept less than 10^{16} molecules.[2] This pulse size is very small compared to the number of sorption sites on the catalyst, as confirmed by the absence of any pulse dependence of the pulse response. It was checked that the tail of each pulse response reached the background before injecting the next pulse. Thereafter, 4–15% of argon was added as an internal standard in the pulse experiments in order to calculate conversions. After some pre-pulses, 150 to 250 pulses were averaged to increase the signal-to-noise ratio in the response. Prior to the experiments, the catalyst was heated at 473 K for 30 min in vacuum to clean the surface from adsorbed species. Then, after this treatment, the temperature of the catalyst was set to the given temperatures (298, 373, and 473 K).

Results and Discussion

Gas Transport. Since the analytical model used by us in order to determine the adsorption/desorption parameters of CO, O_2, and CO_2 assumes a Knudsen flow, at first the validity of this assumption has been verified. Ar single-pulse experiments were carried-out at three temperatures: 298, 373, and 473 K. The pulse size was around 1×10^{15} molecules/pulse (low value) and 6×10^{15} molecules/pulse (high value).

In the Knudsen regime, the product pulse shape should be independent of pulse intensity. To verify this , we have compared the experimental curves obtained for the low pulse intensity and the high pulse intensity, where the comparison is possible only for normalized flows. We have normalized all the Ar experimental curves by dividing the exit flow by the zero-th moment, m_0, which is directly proportional to the number of molecules in the initial pulse.

When irreversible adsorption or reaction occurs, the experimental curve cannot be transformed into a normalized flow using the unit-area-normalization. In this case, the reactant can be calibrated against an inert gas in a separate non-reaction experiment, and the relative calibration factor can be used to transform the reaction experimental response into a normalized flow.[25]

By the normalization of the Ar original curves, we have obtained an unique diffusion curve for each temperature (Fig. 1).

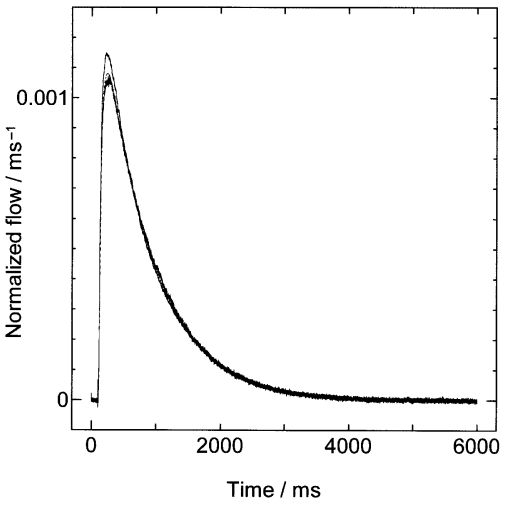

Fig. 1. Unit-area-normalized Ar response curve at 298 K (· · · · · ·), 373 K (- - - -), and 473 K (——).

In order to perform the statistical analysis of our data, we need to set the sampling time. Usually, the time needed in each experiment to reach the background is taken as sampling time. However, the tails of some experimental curves are very long. The questions are: Have these long tails any significance in our data? and can these tails be cut without significantly affecting the physical meaning of statistical parameters (i.e. residence time and dispersion)? In order to give an answer to these questions, we have checked the test of hypothesis[46] for each of cases and we have determined the proper sampling time. This was between 4000 and 5000 ms.

Since the residence time at each temperature did not depend on the pulse intensity, it means that another criterion for Knudsen diffusion is satisfied. In a diffusion-controlled process, the diffusion rate is directly proportional to the velocity of the diffusing species. So, if we plot the average residence time as a function of square root of temperature, the plot should be a straight line. Indeed, we have obtained a straight line whose equation was: t_{res} (ms) = 4.08 $T^{1/2}$ + 735.92 and the correlation coefficient was $R^2 = 0.9973$.

The Knudsen regime can also be confirmed by measuring the peak time and the height of the normalized peak flow. Equation 17 for Knudsen diffusion predicts that the product of the peak time and the normalized peak height is equal to 0.31. As the values calculated for $(H_p t_p)$ from the experimental data are close to the theoretical value (the error was less than 3% for each temperature) we can conclude that Knudsen regime has been confirmed.

Another way of characterizing the Knudsen diffusion regime is to compare the normalized experimental flow with the unique peak-normalized plot (standard normalized flow), described by Eq. 15. In order to do this we have to determine the parameters D_{eAr} and ε_b. We can calculate the effective Knudsen diffusivity for Ar using either Einstein's equation:

$$t_{res} = \frac{L^2 \varepsilon_b}{2 D_{eAr}} \tag{25}$$

or the equation for the peak height (Eq. 17). As the porosity of catalyst bed is unknown , it can be determined from experimental measurements, using the following equation:

$$\varepsilon_b = V_{pore}\rho_{ap}, \quad (26)$$

where $V_{pore} = 161.2\ mm^3\ g^{-1}$ (35) and $\rho_{ap} = 1.4232\ g\ cm^3$ (value determined from the relative apparent density against water, at room temperature, by using a piknometer). Table 1 shows that the diffusivity slightly decreases with temperature, which means that porosity probably slightly changes with temperature. Let's verify this by using another way to calculate the effective diffusivity, from the following equation[47]:

$$D_{eAr} = \frac{\varepsilon_b}{\tau_b} D_{Ar}, \quad (27)$$

where τ_b means the tortuosity of catalyst bed and D_{Ar} is the theoretical Knudsen diffusion coefficient for argon, calculated from:

$$D_{Ar} = \frac{2\overline{r}}{3}\sqrt{\frac{8TR}{\pi M}}. \quad (28)$$

For more or less spherical particles, the interparticle distance is:

$$\overline{r} = \frac{2\varepsilon_b}{3(1-\varepsilon_b)} r_p, \quad (29)$$

and:

$$\tau_b = \frac{a}{\varepsilon_b}. \quad (30)$$

The constant a can take the value 0.1–1, and usually, $\tau_b = 2$–6.[47] Then,

$$D_{eAr} = \frac{2}{3}\frac{\varepsilon_b^2}{a}\frac{2\varepsilon_b}{3(1-\varepsilon_b)} r_p \sqrt{\frac{8TR}{\pi M}}. \quad (31)$$

Using an iteration procedure, for an average particle radius, $r_p = 5.094 \times 10^{-6}$ m, and for $a = 1$, $\varepsilon_b = 0.227$ at room temperature, then ε_b is almost 0.229, like the value from the experimental measurements. We can recalculate now the porosity, tortuosity, and effective diffusion coefficient for argon (Table 2). The results suggest that ε_b changes little with temperature.

If one uses these values for porosity and diffusivity, the simulation of the theoretical curve for argon diffusion is now possible. Figure 2 presents the experimental response curves at

Table 1. Effective Knudsen Diffusion Coefficient for Ar and Porosity of Catalyst Bed

Temp	Resid. time	D_{eAr}/ε_b[a)]	D_{eAr}/ε_b[b)]	D_{eAr}/ε_b(av)	ε_b	D_{eAr}
K	s	$cm^2\ s^{-1}$	$cm^2\ s^{-1}$	$cm^2\ s^{-1}$		$cm^2\ s^{-1}$
298	0.806	0.620	0.612	0.616		0.141
373	0.815	0.613	0.613	0.613	0.229	0.140
473	0.823	0.607	0.601	0.604		0.138

a) Eq.27; b) Eq.16.

Table 2. Changes in the Catalyst Bed Porosity and Tortuosity and the Ar Effective Knudsen Diffusion Coefficient with Temperature

Temp/K	ε_b	τ_b	$D_{eAr}/cm^2\ s^{-1}$
298	0.227	4.41	0.139
373	0.229	4.36	0.140
473	0.234	4.27	0.141

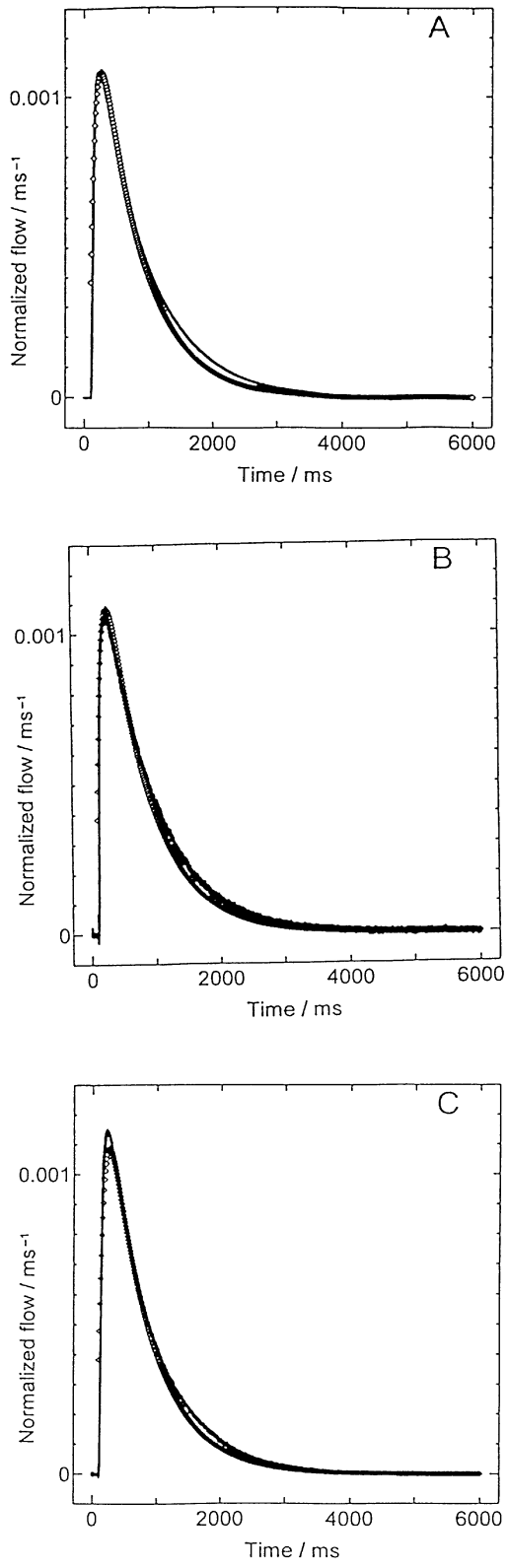

Fig. 2. Experimental (—) and simulated (◇) Ar response curves at (A) 298 K, (B) 373 K, and (C) 473 K.

three temperatures as well as the theoretical ones, simulated by using Eq. 15. The two curves have almost perfectly matched each other. (We have calculated the sum of squares (SS) of the difference between the observed and calculated value. Because the value of this sum was extremely low, no optimization procedure was needed in order to determine the optimum value for the parameters in the model, D_{eAr} and ε_b). It means that the transport mechanism fits perfectly the Knudsen flow.

Now, one can determine the diffusion and adsorption/desorption parameters for CO, O_2, and CO_2 on the Au/Ti(OH)$_4$* catalyst.

Effective Knudsen Diffusivity and Adsorption Parameters for CO. First, we have to determine the adsorption type (reversible or irreversible) and then, we can determine the kinetic parameters. In Fig. 3, which shows the normalized experimental response curves for Ar and CO, the CO TAP curves intersect the Ar curve. This is a fingerprint for reversible adsorption on the surface. The same conclusion was drawn from the statistical analysis of moments. Before normalizing the response curves, we considered the balance of CO against Ar (internal standard). We calculated the mean Ar/CO ratios, from experiments without catalyst. These were 1:22.4 (4.25% Ar, 95.75% CO) at 298 K, 1:22.9 at 373 K, and 1:22.5 at 473 K. Then, we applied the correction factors for the experiments with catalyst. Using the m_0 of the Ar response curve in the presence of catalyst and the correction factors, we calculated the m_0 for a theoretical CO response curve and we compared it with the m_0 of the experimental CO response curve. There was no difference between the theoretical m_0 and the experimental one. Such a result means that CO reversibly adsorbs on the catalyst surface.

Therefore, we can now calculate the kinetic parameters, assuming first-order adsorption and desorption kinetics. Using Eq. 9, we could determine the k_{aCO}/k_{dCO} ratio, but first of all, we need to know the value for effective Knudsen diffusion coefficient for CO, D_{eCO}. From the following Eq. 32,

$$D_{eCO} = D_{eAr}(M_{Ar}/M_{CO})^{1/2} \tag{32}$$

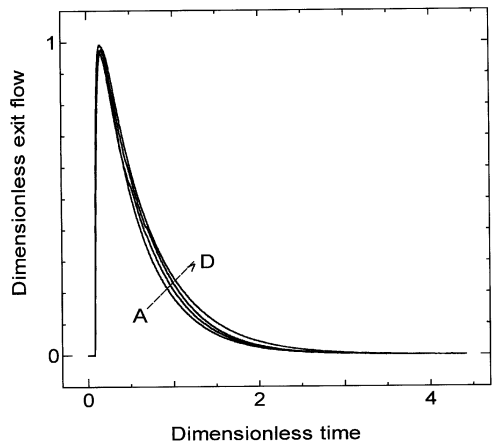

Fig. 3. CO and Ar TAP curves on the Au/Ti(OH)$_4$* catalyst; CO: (A) 298 K, (B) 373 K and (C) 473 K, Ar: (D)

D_{eCO} is: 0.167 cm^2 s^{-1} (298 K), 0.168 cm^2 s^{-1} (373 K), and 0.169 cm^2 s^{-1} (473 K).

From Eq. 11 we determined the value of k_{dCO}, and from the Arrhenius plot the adsorption and desorption activation energies were determined. Table 3 shows the results regarding to the k_{aCO}/k_{dCO}, k_{aCO}, k_{dCO}, adsorption activation energy and desorption activation energy.

The heat of adsorption was obtained to be 2.5 kJ mol^{-1} from the van't Hoff plot of the equilibrium constant, $K = k'_{aCO}/k_{dCO}$, or 2.6 kJ mol^{-1} from the difference $E_{ads} - E_{des}$.

The shape of the CO pulse response was independent of the pulse size, as shown in Fig. 4, which proves that the adsorption and desorption processes are first order with respect to the gas phase concentration of CO, and the concentration of adsorbed CO. As the adsorption and desorption activation energies were low and the CO response curve was almost the same as the Ar one, we can conclude that CO adsorption on the surface is weak. Since the response curves for CO were not broadened, compared to the inert argon response curve, a Langmuir isotherm could be used to describe the CO adsorption process on the Au/Ti(OH)$_4$* catalyst.

Effective Knudsen Diffusivity and Adsorption Parameters for O_2. First, we calculated the effective Knudsen diffusion coefficient for O_2 by multiplying the diffusivity of argon with the square root of the ratio of the argon to the oxygen molecular weight. We obtained the following values: 0.156 (298 K), 0.157 (373 K), and 0.158 cm^2 s^{-1} at 473 K, respectively. In order to normalize the O_2 response curves (dividing the experimental curves by the calculated zero-th moment), we calculated the ratio between Ar and O_2 at different temperatures, from experimental curves without catalyst. The ratios were: 1:5.82 at 298 K, 1:6.25 at 373 K, and 1:6.29 at 473 K. Figure 5 presents the normalized curves for large pulse intensities. The results indicate an irreversible adsorption of O_2 on the surface. In this case, the flow curve is located inside the standard Ar diffusion curve. Indeed, the mean values for the zero-th moments at 298 K, 373 K, and 473 K, for the O_2 normalized response curves were less than unity at the three temperatures. Such a rersult means that O_2 irreversibly adsorbs on the surface.

Using Eq. 24, we obtained the mean values for the conversion of O_2 for large pulse intensities. There is another way to calculate the amount of oxygen irreversibly adsorbed on the surface, and then the conversion. This amount is directly proportional to the difference between the theoretical zero-th moment of oxygen response curves, $m_0{}'_{O_2,calc}$ (calculated by multiplying the zero-th moment of Ar response curve, $m_0{}'_{Ar}$ with the ratio between Ar:O_2 in the initial mixture) and the experimental zero-th moment curves, , $m_0{}'_{O_2,exp}$. The O_2 conver-

Table 3. Kinetic Parameters for CO Adsorption on Au/Ti(OH)$_4$*

Temp	Resid. time	k'_{aCO}/k_{dCO}	k'_{aCO}	k_{dCO}	E_{ads}	E_{des}
K	s		s^{-1}	s^{-1}	kJ mol^{-1}	kJ mol^{-1}
298	0.720	0.059	0.014	0.24		
373	0.735	0.076	0.021	0.28	4.6	1.4
473	0.770	0.087	0.026	0.30		

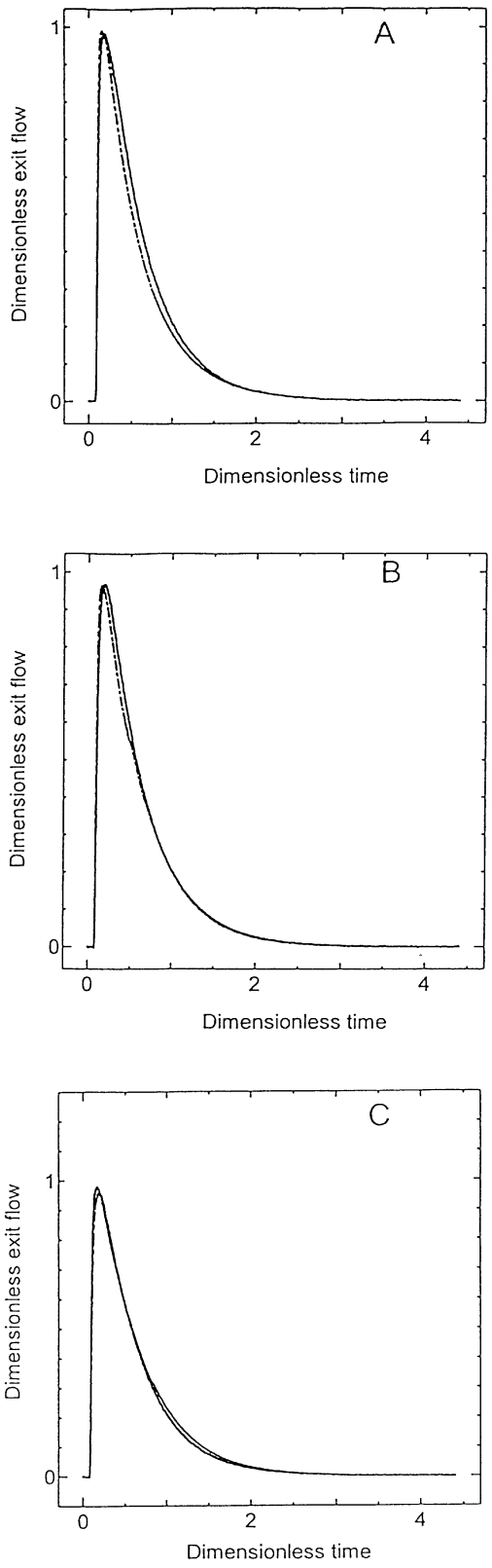

Fig. 4. Carbon monoxide responses with the two different pulse sizes at (A) 298 K, (B) 373 K and (C) 473 K. ——: High pulse intensities. –•–: Low pulse intensities.

sion presents a maximum at 373 K. We know that this catalyst appreciably increases the amount of oxygen adsorbed on the

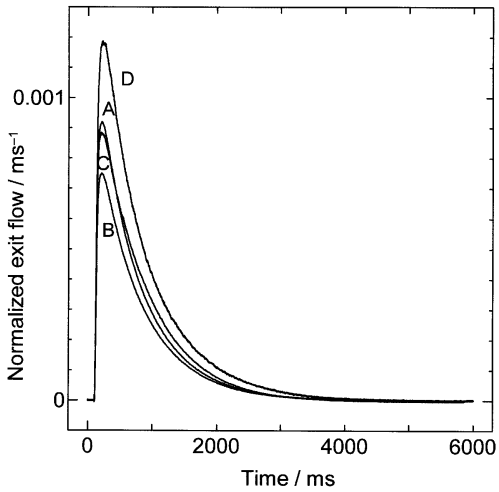

Fig. 5. Irreversible adsorption of oxygen on Au/Ti(OH)$_4$* for large pulse intensities at (A) 298 K, (B) 373 K, (C) 473 K, and (D) Ar pulse response as reference.

support oxides.[48] But this has been verified from the present TAP experiments only for the temperatures equal to or less than 373 K.

For small pulse intensities, the mean values of $m_{0\,O_2,exp}$ at the three temperatures were a little bigger than those of $m_{0\,O_2,calc}$. It means, for this pulse size, that the O_2 adsorption is reversible.

Therefore, we have to calculate separately the adsorption parameters for large pulse intensities as well as for small pulse ones.

(A) Irreversible Adsorption. Assuming a first order adsorption/reaction kinetics, in other words, assuming that oxygen molecularly adsorbs on the surface, and using Eq. 23, we calculated the adsorption rate constant, and from Eq. 24 the conversion. Table 4 shows these calculated values. Very roughly we calculate a positive apparent adsorption activation energy, 10.1 kJ mol^{-1} from room temperature to 373 K, while a negative one, –15.1 kJ mol^{-1} is found at 373–473 K.

In order to verify what happened between 373 and 473 K, we examined each successive experiment at 473 K. Therefore, we calculated the Ar/O_2 ratio, $m_{0\,O_2,calc}$, X_{O_2} from the difference between $m_0'_{O_2,calc} - m_0'_{O_2,exp}$ (Δ), and X_{O_2} from $1 - m_{0\,O_2}$ (normalized flow) as shown in Table 5. Indeed, the amount of O_2 irreversibly adsorbed on the surface decreases at 473 K, from experiment to experiment. We thought that it was possible because from experiment to experiment the concentration of O_2 adsorbed on the surface increases and so the O_2

Table 4. Influence of Temperature on Conversion and on Apparent Adsorption/Reaction Rate Constant of O_2 over Au/Ti(OH)$_4$*

Temp/K	m_0(normalized flow)	k'_{aO_2}/s^{-1}	X_{O_2}/%
298	0.87	0.192	12.16
373	0.74	0.435	25.12
473	0.89	0.153	10.40

Table 5. Result of the Kinetic Analysis of O_2 Responses at 473 K

Expt.no.	Ar/O_2	$m_{0\ O_2 calc}$	Δ	$X_{0_2}/\%$	$m_{0\ O_2}$ (normalized flow)	$X_{O_2}/\%$
1	1:6.3	540.49	105.78	19.57	0.804	19.62
2	1:6.4	459.85	58.14	12.64	0.874	12.64
3	1:6.5	405.49	13.21	3.25	0.967	3.32

desorption becomes more probable than adsorption.

In order to verify if O_2 adsorption is dissociative or associative on this catalyst, first we compared the O_2 experimental response curves with the simulated O_2 molecular irreversible adsorption curve by using Eq. 20. As shown in Fig. 6, there is an almost perfect fitting between the two curves. The results demonstrate that O_2 molecularly adsorbs on the catalyst surface, in agreement with our previous study on active oxygen species on the $Au/Ti(OH)_4$* catalyst.[41]

There is another way to verify the type of O_2 adsorption. Using the calculated value for the adsorption rate constant at three temperatures, we can calculate the first moment of theoretical (supposing a molecular adsorption) dimensionless exit flow, m_{1d}, and then we can compare it with the first moment calculated by statistical analysis (from the experimental response curves):

$$m_{1d} = \pi \sum_{n=0}^{\infty} \frac{(-1)^n(2n+1)}{((n+0.5)^2\pi^2 + k_{aO_2d})^2} \tag{33}$$

where

$$k_{aO_2d} = \frac{k'_{aO_2}\varepsilon_b L^2}{D_{eO_2}}. \tag{34}$$

On the other hand,

$$m_{1d} = \frac{m_1 D_{eO_2}}{\varepsilon_b L^2}. \tag{35}$$

As the errors are less then 5%, we can conclude that O_2 molecularly adsorbs on the catalyst surface.

The desorption kinetics should be second order if dissociative adsorption of oxygen occurs.

(B) Reversible Adsorption. In order to analyze the experimental data in the case of low pulse intensities, we normalized the experimental curves. One example of normalized curve, obtained by dividing the experimental O_2 response curve with the number of molecules/pulse (which is directly proportional to the zero-th moment of experimental curve multiplied by a correction factor, obtained from the balance against Ar) is presented in Fig. 7. First, from Eq. 9 we obtained the ratio k'_{aO_2}/k_{dO_2}. Then, using Eq. 11 we obtained k_{dO_2}. Assuming an Arrhenius temperature dependence for k'_{aO_2} and k_{dO_2}, we can find the apparent adsorption activation energy as well as the apparent desorption activation energy. The results are shown in the Table 6.

In conclusion, the adsorption of oxygen on this catalyst can be described by the following model:

$$O_2 + Y \Leftrightarrow O_2Y \xrightarrow{+e^-} O_2{}^-Y \tag{36}$$

At low pulse intensities (that means low gas phase concentration of oxygen) only a reversible physical adsorption occurs. In this case, the oxygen adsorbed species could be considered as a mobile precursor for the oxygen chemisorption. If a molecule adsorbs in the precursor state, it may (i) become chemisorbed, (ii) be inelastically scattered back into the gas phase, or (iii) hop to a neighboring site, in which case pathways (i) and (ii) are again open. The desorption rate is larger than the adsorption rate, reflecting the fact that the activation energy for the desorption was smaller than that for the adsorption. For high pulse intensities, the oxygen chemisorption becomes competi-

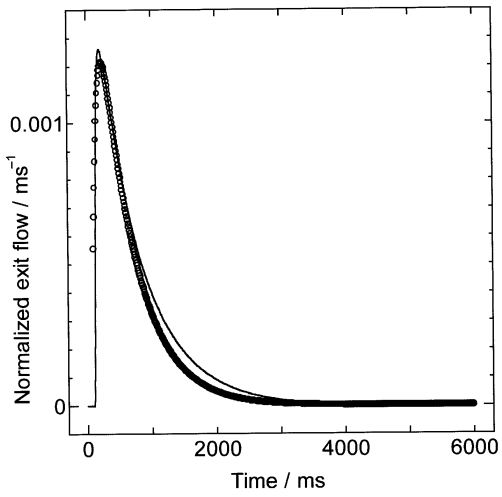

Fig. 6. Experimental (solid line) and model-predicted (open circles) transient response for O_2 on $Au/Ti(OH)_4$* at 298 K.

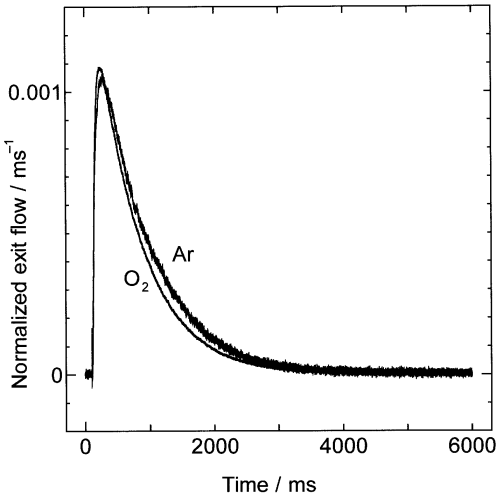

Fig. 7. Normalized low intensity O_2 response and Ar response as reference at 298 K.

Table 6. Kinetic Parameters for Reversible Adsorption of Oxygen

Temp/K	Resid. time/s	k'_{aO_2}/k_{dO_2}	$k_{aO_2}\times10^3/s^{-1}$	k_{dO_2}/s^{-1}	E_{ads}/kJ mol^{-1}	E_{des}/kJ mol^{-1}
298	0.741	0.019	1.475	0.075		
373	0.749	0.026	2.658	0.102	8.2	3.8
473	0.769	0.038	5.007	0.132		

tive with the oxygen desorption.

Now, we can conclude that for the pulse size around 1×10^{16} molecules/pulse the observed oxygen response curves fitted very well with the theoretical irreversible-adsorption curve simulated by a model involving no dissociative adsorption of oxygen. However, the TAP single-pulse experiments performed at three different temperatures reveal an interesting behavior of oxygen during the adsorption on the active Au/Ti(OH)$_4$* catalyst. If we analyze the dimensionless response curves for the three temperatures, we observe that the response curves for low temperatures (equal to or less than 373 K) are sharper than that for 473 K (Fig. 8). The curves for the low temperatures were expected to be broadened, because at the high temperature the desorption may be faster. This behavior could be explained as follows. At a high temperature, the dissociation of O_2 on the surface is possible, followed by the recombination of the produced atomic oxygen and then by the desorption. The rate of the recombination seems to be slower than the rate of the desorption.

Moreover, for low pulse size intensities (about 1×10^{15} molecules/pulse) there are no differences in the O_2 response curves at the three temperatures. It means that for low O_2 gas-phase concentration and for low O_2 adsorbed concentration, the desorption reaction is more probable than dissociation and recombination. We can explain why the adsorption rate of O_2 decreases at high temperature. At the high temperature, two parallel oxygen adsorption processes occur: an irreversible molecular adsorption and a dissociative adsorption. In this way, the selectivity decreases, and the conversion of O_2 as O_2^- (the active species in CO oxidation[41]) is less than the one at the lower temperatures. The TAP studies confirm a weak and reversible adsorption, as previous studies reported.[41,49]

Effective Knudsen Diffusivity and Adsorption Parameters for CO_2 on Au/Ti(OH)$_4$*. We assumed that adsorption/reaction was of first order kinetics. Figure 9 indicates an irreversible adsorption/reaction of CO_2 on the surface, because the CO_2 normalized response curves are inside of Ar ones. CO_2 seems to strongly adsorb on the catalyst surface. Indeed, there was a large difference between the m_0 from the statistical analysis of experimental data and the m_0 calculated from the balance against Ar. This large difference is directly proportional to the CO_2 conversion. Let's calculate this conversion by using the difference and Eq. 23. Table 7 shows the values for the con-

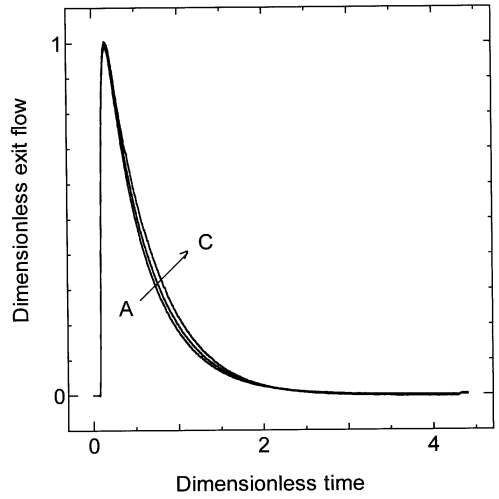

Fig. 8. Temperature influence of the TAP response on the irreversible adsorption of oxygen on Au/Ti(OH)$_4$* at (A) 298 K, (B) 373 K, and (C) 473 K.

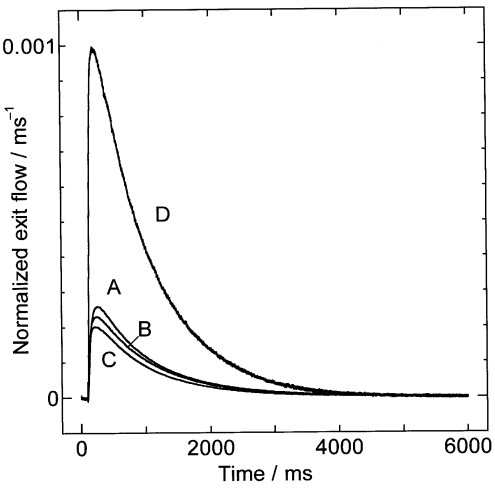

Fig. 9. Normalized CO_2 response at (A) 298 K, (B) 373 K, and (C) 473 K and (D) Ar pulse response as reference.

Table 7. Kinetic Parameters for CO_2 Irreversible Adsorption over Au/Ti(OH)$_4$*

Temp/K	X_{CO_2}(from difference)/%	X_{CO_2}(from Eq. 23)/%	k'_{aCO_2}/s^{-1}	E_{ads}/kJ mol^{-1}
298	79.36	80.70	3.18	
373	79.48	79.51	3.01	−0.3
473	79.29	79.33	2.99	

version along with the kinetic parameters. The adsorption activation energy is almost zero and the adsorption rate constant is very large. It means that CO_2 adsorption is very fast. To verify if CO_2 adsorption/reaction is indeed first order with respect to gas phase CO_2 concentration and adsorbed CO_2 concentration, we compared the experimental normalized response curves with the simulated adsorption/reaction curve, as Eq. 20 predicts.

The experimental response curves for the two pulse sizes are broader than the simulated curve. This difference could be due to the saturation of active sites or to the fact that are not first order kinetics. (The squared deviation of normalized exit flow values between the predicted model and the experimental ones, was 7.5×10^{-8} for high pulse intensities and 8.6×10^{-8} for low pulse intensities, respectively). But, we observed that the two experimental curves almost perfectly fitted each other. This is the proof for first-order kinetics. Therefore, to demonstrate that the site saturation caused the differences, we calculated the conversion for some successive experiments at 298 K, for high pulse intensities as well as for low pulse intensities. The conversion increased from experiment to experiment (75.4%, 77.6%, 79.9%, and 81.8%) for high pulse intensities, while for the low pulse intensities, the conversion is almost constant (80.9%, 80.2%, 80.0%, 80.0%). Thus, in the case of high intensities, (high CO_2 gas-phase concentration), the probability of CO_2 adsorption and then reaction on the surface to form carbonate species is higher than in the case of low pulse intensities. As the experimental response curves are still broad, CO_2 response is due not to desorption but to carbonate decomposition reaction, which is a slow step on the surface. On the other hand, the site saturation should induce a delay in the TAP response. Indeed, if we divided the time of the experimental curves with the ratio between t_p for the experimental curves and t_p for the model-predicted response, the fitting was much better (Fig.10).

In contrast to the cases of CO and O_2, CO_2 strongly and irreversibly adsorbs on the surface as carbonate-like species. O_2 adsorption is slower than CO and CO_2 adsorption. The O_2 adsorption can be a rate determining step for CO oxidation on the $Au/Ti(OH)_4$* catalyst.

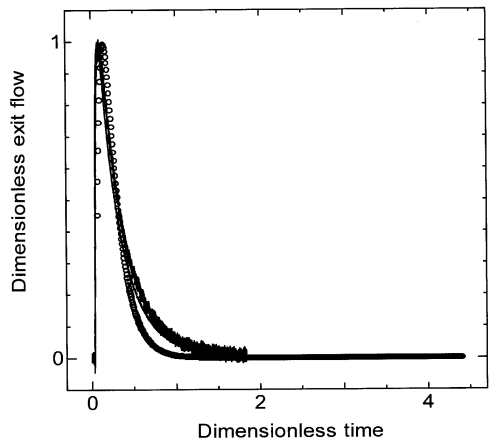

Fig. 10. TAP response for CO_2 adsorption/reaction on $Au/Ti(OH)_4$*; Model-predicted: open circles. High pulse intensities: dash line. Low pulse intensities: solid line.

Conclusion

In order to sustain the previously reported CO oxidation mechanism on a $Au/Ti(OH)_4$* catalyst,[41] the adsorption of CO, O_2, and CO_2 was studied by means of single pulse experiments in a TAP reactor. A qualitative interpretation (by comparison of the experimental response curves of species of interest with Ar response curves) as well as a quantitative one (based on a statistical approach as well as a deterministic one) have been done for the experimental response curves. A first-order adsorption/desorption kinetics, for all species of interest, leads to an excellent matching between experimental and theoretical results. The TAP analysis indicates that CO adsorption on $Au/Ti(OH)_4$* is reversible and O_2 adsorbs molecularly and reversibly for low pulse intensities. For high pulse intensities O_2 also adsorbs molecularly, but irreversibly. CO_2 always adsorbs irreversibly under the TAP conditions.

Notation

a	constant
a_s	surface concentration of active sites (mol cm^{-2} of catalyst)
A	cross-sectional area of the reactor (cm^2)
C_A	concentration of gas A (mol cm^{-3})
D_{eA}	effective Knudsen diffusivity of gas A (cm^2 s^{-1})
E_a	apparent activation energy (kJ mol^{-1})
F_A	flow of gas A at the reactor outlet (mol s^{-1})
H_p	peak height of the normalized exit flow (s^{-1})
k_a	adsorption rate constant (cm^3 of gas mol^{-1} s^{-1})
k'_a	apparent adsorption rate constant (s^{-1})
$\bar{k}_a$	dimensionless adsorption rate constant defined by Eq. 22
k_d	desorption rate constant (s^{-1})
k_r	reaction rate constant
L	length of the reactor (cm)
n	index of infinite series
m_i	ith moment of normalized exit flow
m'_i	ith moment of exit flow
M	molecular weight (g mol^{-1})
N_{pA}	number of molecules of A in the inlet pulse
r_p	particle radius (cm)
$\bar{r}$	mean interparticle distance (cm)
R	molar gas constant (J mol^{-1} K^{-1})
S_v	surface area of catalyst per volume of catalyst (cm^{-1})
t	time (s)
t_p	time at which the exit flow is at a maximum
t_{res}	mean residence time
T	temperature (K)
x	axial coordinate (cm)
X	conversion (%)
Y	active site

Greek letters

δ_x	delta function with respect to axial coordinate (x)
ε_b	porosity of the bed
ρ_s	concentration of adsorption sites (sites/cm^3 of bed)
θ_A	fractional surface coverage
τ_b	tortuosity of bed

References

1 J. T. Gleaves, J. R. Ebner, U.S. Pat. US 4,626,412 (02.12.1986).

2 J. T. Gleaves, J. R. Ebner, and T. C. Kuechler, *Catal. Rev.Sci. Eng.*, **30**, 49 (1988).

3 G. Creten, D. S. Lafyatis, and G. F. Froment, *J. Catal.*, **154**, 151 (1995).

4 J. T. Gleaves, A. G. Sault, R. J. Madix, and J. R. Ebner, *J. Catal.*, **121**, 202 (1990).

5 G. D. Svoboda and J. T. Gleaves, *Ind. Eng. Chem. Res.*, **31**, 19 (1992).

6 G. Golinelli and T. J. Gleaves, *J. Mol. Catal.*, **73**, 353 (1992).

7 J. T. Gleaves and G. Centi, *Catal. Today*, **16**, 69 (1993).

8 B. Kartheuser, B. K. Hodnett, H. W. Zanthoff, and M. Baerns, *Catal. Lett.*, **21**, 209 (1993).

9 O. V. Buyevskaya, M. Rothaemel, H. W. Zanthoff, and M. Baerns, *J. Catal.*, **150** 71 (1994).

10 Y. Schuurman and J. T. Gleaves, *Ind. Eng. Chem. Res.*, **33**, 2935 (1994).

11 Y. J. Mergler, J. Hoebink, and B .E. Nieuwenhuys, *J. Catal.*, **167**, 305 (1997).

12 G. Creten, F. D. Kopinke, and G. F. Froment, *Canadian J. Chem. Eng.*, **75**, 882 (1997).

13 A. Pantazidis, S. A. Bucholz, H. W. Zanthoff, Y. Schuurman, and C. Mirodatos, *Catal. Today*, **40**, 207 (1998).

14 K. H. Hofstad, J. H. B.J. Hoebink, A. Holmen, and G.B. Marin, *Catal. Today*, **40**, 157 (1998).

15 T. Gerlach and M. Baerns, *Chem. Eng. Sci.*, **54**, 4379 (1999).

16 O. Dewaele, V. L. Geers, G. F. Froment, and G. B. Martin, *Chem. Eng. Sci.*, **54**, 4385 (1999).

17 D. Creaser, B. Andersson, R. R. Hudgins, and P. L. Silveston, *Appl. Catal., A*, **187**, 147 (1999).

18 A. Hinz and A. Andersson, *Chem. Eng. Sci.*, **54**, 4407 (1999).

19 O. Dewaele, D. Wang, and G. F. Froment, *J. Mol. Catal. A: Chem.*, **149**, 263 (1999).

20 O. Dewaele and G. F. Froment, *Apll. Catal. A*, **185**, 203 (1999).

21 E. V. Kondratenko, O. V. Buyevskaya, M. Soick, and M. Baerns, *Catal. Lett.*, **63**, 153 (1999).

22 B. Zou, M. P. Dudukovič , and P. L. Mills, *Chem. Eng. Sci.*, **48**, 2345 (1993).

23 B. Zou, M. P. Dudukovič , and P. L. Mills, *J. Catal.*, **145**, 683 (1994).

24 M. Rothaemel and M. Baerns, *Ind. Eng. Chem. Res.*, **35**, 1556 (1996).

25 J. T. Gleaves, G. S. Yablonskii, P. Phanawadee, and Y. Schuurman, *Appl. Catal. A*, **160**, 55 (1997).

26 D. Lafyatis, G. Creten, O. Dewaele, and G. F. Froment, *Can. J. Chem. Eng.*, **75**, 1100 (1997).

27 G. S. Yablonskii, I. N. Katz, P. Phanawadee, and J. T. Gleaves, *Ind. Eng. Chem. Res.*, **36**, 3149 (1997).

28 G. S. Yablonskii, S. O. Shekhtman, S. Chen, and J. T. Gleaves, *Ind. Eng. Chem. Res.*, **37**, 2193 (1998).

29 S. O. Shekhtman, G. S. Yablonskii, S. Chen, and J. T. Gleaves, *Chem. Eng. Sci.*, **54**, 4371 (1999).

30 T. A. Nijhuis, L. J. P. van den Broeke, M. J. G. Linders, J. M. van de Graaf, F. Kapteijn, M. Makkee, and J. A. Moulijn, *Chem. Eng. Sci.*, **54**, 4423 (1999).

31 P. Phanawadee, Ph.D. dissertation, Washington University, St. Luis, Mo (1997).

32 Y. Yuan, K. Asakura, H. Wan, K. Tsai, and Y. Iwasawa, *Chem. Lett.*, **1996** 755.

33 Y. Yuan, A. P. Kozlova, K. Asakura, H. Wan, K. Tsai, and Y. Iwasawa, *J. Catal.*, **170**, 191 (1997).

34 A. P. Kozlova, S. Sugiyama, A. I. Kozlov, K. Asakura, and Y. Iwasawa, *J. Catal.*, **176**, 426 (1998).

35 A. I. Kozlov, A. P. Kozlova, H. C. Liu, and Y. Iwasawa, *Appl. Catal. A*, **182**, 9 (1999).

36 F. Boccuzzi, A. Chiorino, S. Tsubota, and M. Haruta, *J. Phys. Chem.*, **100**, 3625 (1996).

37 M. Haruta, S. Tsubota, T. Kobayashi, H. Kageyama, M. J. Genet, and B. Delmon, *J. Catal.*, **144**, 175 (1993).

38 M. Haruta, *Catal. Today*, **36**, 153 (1997).

39 M. Haruta, *Catal. Surv. Jpn.*, **1**, 61 (1997).

40 F. Boccuzzi, E. Guglielminotti, F. Pinna, and G. Strukul, *Surf. Sci.*, **377-379**, 728 (1997).

41 H. Liu, A. I. Kozlov, A. P. Kozlova, T. Shido, K. Asakura, and Y. Iwasawa, *J. Catal.*, **185**, 252 (1999).

42 G. C. Bond and D. T. Thompson, *Catal. Rev. Sci. Eng.*, **41**, 319 (1999).

43 T. A. Nijhuis, L. J. P. van den Broeke, M. J. G. Linders, M. Makkee, F. Kapteijn, and J. A. Moulijn, *Catal. Today*, **53**, 189 (1999).

44 B. Zou, N. Rigas, P. L. Mills, J. T. Gleaves, and M. P. Dudukovič , Proc. of AIChE 1988 Annual Meeting, Symposium on Novel Reactors for Heterogeneous Systems.

45 J. Huinink, Ph.D. dissertation, Eindhoven University of Technology, Eindhoven, The Netherlands (1995).

46 Mc Graw-Hill Handbooks, Lange's Handbook of Chemistry, Fifteen Edition, ed by John A. Dean, (1999), Vol. 2, P. 117.

47 D. G. Huizenga and D. M. Smith, *AIChE J.*, **32**, 1 (1986).

48 E. D. Park and J. S. Lee, *J. Catal.*, **186**, 1 (1999).

49 H. Liu, A. I. Kozlov, A. P. Kozlova, T. Shido, and Y. Iwasawa, *Phys.Chem. Chem. Phys.*, **1**, 2851 (1999).